Available online www.ejaet.com

European Journal of Advances in Engineering and Technology, 2024, 11(3):106-114

Research Article ISSN: 2394 - 658X

Evaluation of performance parameters of a shell and tube heat exchanger: A theoretical study

Shreyas Kotian[a], Nishant Jain[b], Nachiket Methekar[c], and Pranit Vartak[b]

[a]Department of Mechanical and Aerospace Engineering, University of California- San Diego, San Diego, CA, 92093, USA

[b]Department of Mechanical Engineering, K.J. Somaiya College of Engineering, Mumbai 400077, India

[c]Department of Industrial Engineering and Management Sciences, Northwestern University, Evanston, IL, 60208, USA

ABSTRACT

Shell and tube heat exchangers (STHX) have assumed importance over the years due to their great versatility. For the evaluation of STHX, thermal performance, and pressure drop are considered as major factors. These factors are dependent on the inlet conditions, flow conditions, and tube and shell geometry. The present study analyzes the theoretical calculations for the evaluation of performance parameters of the STHX at various inlet temperatures of the hot fluid and flow conditions. It was observed that the overall heat transfer coefficient and the tube side pressure drop increased with an increase in the Re number of the hot fluid. The effectiveness and NTU show similar trends, decreasing first attaining a minimum, and increasing again.

Key words: Shell and tube heat exchanger, analytical study, performance parameters.

Nomenclature

u_m	mean velocity of fluid [m/s]	m_h	mass flow rate of hot fluid [kg/s]
C_{max}	maximum heat capacity of fluid [W/K]	m_c	mass flow rate of cold fluid [kg/s]
C_{min}	minimum heat capacity of fluid [W/K]	h	heat transfer coefficient[W/m^2-K]
C_p	heat capacity [J/kg-K]	A	heat transfer area [m^2]
N_t	number of Tubes	G	channel mass velocity [kg/m^2-s]
d_i	inner diameter of tube [mm]	NTU	number of transfer units
d_o	outer diameter of tube [mm]	Nu	Nusselt Number
D_e	equivalent diameter [mm]	Re	Reynolds Number
L	length of tubes [mm]	T	temperature [K or °C]
Pe	Peclet number	U_c	overall heat transfer coefficient for clean surface [W/m^2-K]
Δp	pressure drop [Pa]	f	fanning friction factor
N_p	number of passes	k	thermal conductivity [W/m-K]
$\dot{m}$	mass flow rate of fluid [kg/s]	Pr	Prandtl number
Q	heat transfer rate [W]	Δp_t	Tube side pressure drop
h_{id}	heat transfer coefficient for pure cross flow in an ideal tube bank	N_{cw}	the number of tube rows crossed in the baffle window
ε	effectiveness	N_c	the total number of tube rows crossed in the exchanger
j_i	Colburn j factor for an ideal tube bank	N_{cw}	the number of tube rows crossed in the baffle window
N_b	Number of baffles	C_c	Heat capacity of cold fluid
Δp_s	Shell side pressure drop	T_{h_o}	Outlet temperature of the hot fluid
C_h	Heat capacity of hot fluid	T_{c_o}	Outlet temperature of the cold fluid
C^*	Heat capacity ratio		

1. INTRODUCTION

A heat exchanger is a device that exchanges thermal energy from one fluid to another or from a solid surface to a fluid. They are used in a variety of settings, including industrial, health care, and household. Due to its augmented thermal performance, durable construction, simplicity of maintenance, and upgradeability, shell-and-tube heat exchangers (STHXs) account for more than 30% of heat exchangers used in industrial applications [1]. They have relatively high heat transfer area to volume and weight ratios. They can suit any requirement, such as steam generators, feedwater heaters, pressurized water reactors, or nuclear power plants, thanks to their increased versatility. STHX has the disadvantage of requiring more area than other heat exchangers. Many investigators have investigated the impact of flow conditions and geometrical parameters on the performance characteristics of the STHX using numerical and theoretical analyses. To compare porous and solid baffles, Abbasi et al. [2] ran numerical simulations on STHX. The flow rate was varied and the cold fluid inlet temperature was kept constant at 300K. The thermal and hydraulic characteristics were evaluated, and it was discovered that using porous baffles reduces pressure drop by a great margin while increasing thermal characteristics when compared to solid baffles. The influence of baffle orientation and baffle cut on the performance parameters of the STHX was investigated using numerical simulations by Afsar and Inam [3]. The flow rate was altered while the cold fluid's input temperature was kept at 300K. The working fluid was water, and it was discovered that vertical baffles create superior thermal properties than horizontal baffles, with an augmentation in heat transfer by 10% but with a penalty of a 7% rise in pressure drop. Bicer et al. [4] suggested a new and inventive baffle design to reduce STHX pressure loss while maintaining thermal performance. The hot fluid's input temperature was changed between 338 and 346 K. The three zonal baffles were found to be superior once the design was optimized, with a drop in shell side pressure of 49 percent and a 7 percent increase in shell side temperature. The three zonal baffles increased the heat exchanger's thermal and hydraulic performance, according to the findings. Using numerical simulations, Bichkar et al. [5] studied the effect of baffle type on the thermal performance and pressure drop of an STHX. For the analysis, three different types of baffles were used. Single segmental baffles revealed the presence of recirculation zones, which are responsible for heat transfer. When compared to a single segmental baffle, the double segmental baffle lowers vibrational damage. Due to the elimination of these zones, helical baffles had a 54 percent lower pressure drop and an 88 percent lower pressure drop than double-segmental and single-segmental baffles, respectively. Karno and Ajib [6] created a new computer-aided program for STHX. The impact of various geometrical parameters such as baffle cut, baffle spacing, tube size, and shell size on the performance parameters of the STHX was the focus of this work. The heat exchanger's longitudinal and transverse pitch performance parameters were evaluated in this study. The hot fluid's inlet temperature and the cold fluid’s inlet temperature were kept constant. When the longitudinal and transverse pitches were altered, the value of the local heat transfer coefficient changed. Kim et al. [7] investigated various headers computationally to establish a uniform distribution of gas phase flow in the STHX header. The orientation of the entrance nozzle, the number of outlet tubes, and the length of the heat exchanger were all altered. The regularity of flow distribution rose with header length, but declined with gas flow rate, according to numerical simulations. The simulations could also suggest the best shape and location for the inlet nozzle to provide a consistent flow distribution. Using numerical simulations, Leoni et al. [8] studied the effect of baffle geometry on shell side flow. The SST model outperformed the other turbulence models in terms of accuracy. The shell side fluid's pressure drop and exit temperature were investigated. The outlet temperature of the shell side fluid was discovered to be 8 K higher than the stipulated outlet temperature. It was also shown that when clearances are taken into account in an STHX, the pressure loss is reduced by around 40%. Li et al. [9] investigated the effect of helical baffles in a heat exchanger. The numerical and experimental investigation of baffles with different geometrical aspects were conducted. Water was utilized for the tube side fluid while oil was used for the shell side fluid. The heat exchanger with single-helical baffles had a better ratio of heat transfer coefficient to pressure drop than the single-segmental baffles. As a result, single-helical baffles have better thermal characteristics while using the same amount of pumping force. Mellal et al. [10] tested just how various baffle spacing and orientations affected hydro-thermal shell side performance. The flow rate was adjusted by using 6, 8, and 10 baffles positioned at varying angles. Changes in baffle spacing result in changes in heat exchanger performance, according to computer models. When the baffle spacing is reduced, the thermal and hydraulic characteristics augment. At an angle of 180°, the maximum heat transfer coefficient is achieved because the fluid particles are forced into a haphazard motion which enhances turbulence intensity, boosting the thermal and hydraulic characteristics. On the shell side of a small STHX, Ozden, and Tari [11] ran simulation studies. Water is utilized as the working fluid, with a mass flow rate of 0.5 kg/s on both the hot and cold sides. For each example, different turbulence models were performed and errors were computed. The significance of baffles was also investigated, and it was discovered that baffles are utilized to guide flow within the shell from the intake to the exit while maintaining adequate circulation of the shell side fluid, allowing for efficient heat transfer. The impact of tube arrangement on the thermal performance of an STHX was examined experimentally by Kallannavar et al. [12]. The investigation employed several tube arrangement angles and flow rates ranging from 0.022 kg/s to 0.0045 kg/s. For the 45° tube arrangement, it was determined that the counterflow heat exchanger was 26.7 percent more effective than the parallel flow heat exchanger based on experimental findings. In contrast to the other tube layouts, it was also determined that the 30° tube arrangement had the optimum thermal performance. Mahendran [13] used a floral baffle plate arrangement to conduct an experimental investigation of an STHX. Water was utilized as the working fluid, with varying flow rates. The impact of segmental and floral baffle plates on the heat exchanger's thermal performance was studied, and it was discovered that the flower plate provided the best results. At a flow rate of 17 LPM, the heat exchanger with the flower baffles had a better thermo-hydraulic performance than the heat exchanger with segmental baffles. To assess the effectiveness of STHX, Chen et al. [14] conducted experimental studies with a new unilateral ladder-type helical baffle (ULHB). Under the same flow conditions, STHX with ULHB was compared to STXH with segmental baffles. For different flow rates, the shell side and tube side thermal characteristics were observed to rise by 109.3-125.5 percent and 105.2-122.5 percent, respectively. The STHX's hydraulic performance with ULHB was also improved. Li et al. [15] investigated the thermal-hydraulic performance and energy efficiency of longitudinal flow in STHX using both experimental and computational methods. The working fluid was water, with the volume flow rate on the shell side changing. The equilateral triangle configuration was shown to provide a higher effective heat exchange surface than the square layout, with a 32.81-43.91 percent increase in shell side Nu. It was also discovered that increasing the rod size increased heat transmission from the shell side. The impact of wired nails circular rod inserts on the tube side performance of a shell and tube heat exchanger was investigated experimentally by Marzouk et al. [16]. The working fluid was water, with the tube side flow rate ranging from 13 to 18 LPM and the shell side flow rate being constant. Based on the findings, it was determined that the wired nails significantly improved the STHX's thermal and hydraulic performance. Heat transmission was increased by 210-280 percent and NTU by 132-149 percent, respectively. Kannan and Rudramoorthy [17] investigated the impact of an inlet splitting header on thermohydraulic performance both experimentally and computationally. Both laminar and turbulent flow regimes were studied in simulations. There were two distinct inlet dividing headers employed. When the area ratio of the header was 1.89, the flow rate through the first branch pipe was from 100% to 41% with an increase in Re from 500 to 10,000 respectively. Yang et al. [18] compared an STHX with two shells and continuous helical baffles in the outer shell and segmental baffles in the inner pass (CSTSP-STHX) to an STHX with segmental baffles using experimental and numerical simulations. The earlier arrangement featured a greater shell side heat transfer coefficient as well as a higher value of shell side pressure drop than the latter. At the same mass flow rate, the CSTSP-STHX had a slightly lower heat transfer coefficient per unit pressure drop, but a significantly higher shell side heat transfer coefficient at the same pressure drop. Li and Kottke [19] used mass transfer arrangements to calculate local heat transfer coefficients in STHX with staggered tube configuration. The heat transmission was discovered to be uniformly dispersed across the tube surfaces. The variations in local heat transfer coefficients throughout the circumference of any cross-section of the tube for low Re are considerably higher than the differences along the tube. When Re is low, flow instability develops in the cross-flow and outlet window zones of the tube. Wang et al. [20] conducted an experimental investigation to determine the heat transfer enhancement through the blockage of the triangle leakage zone in a heat exchanger with helical baffles. The flow patterns showed that the helical pitch of streamlines decreases and the velocity vectors both in radial and axial directions increase obviously for the configuration improvement. The experimental results showed an improvement in the thermal characteristics of the heat exchanger. Peng et al. [21] experimented on STHX using both continuous helical and segmental baffles. When the thermal performance of these two heat exchangers was evaluated, it was discovered that STHX with continuous helical baffles increased heat transfer by roughly 10% above STHX with segmental baffles. For continuous helical baffles with various shell configurations, non-dimensional correlations for heat transfer coefficient and pressure drop were also obtained.

2. GEOMETRY OF STHX

Single shell two tube pass shell and tube heat exchanger is used in the present investigation. E-Type shell was selected which is generally used in a single pass shell. Geometric details of the selected configuration of STHX are given in **Table 1**.

Table 1: Geometry of the STHX under investigation

Geometric Parameters	**Magnitude (Unit)/ Description**
Inner Tube Diameter	5.23 mm
Outer Tube Diameter	6.35 mm
Tube Layout	Triangular
Layout Type	Staggered
Layout Angle	30°
Number of Tubes per pass	10
Number of Passes	2
Length of Tube	500 mm
Pitch	7.937 mm
Pitch Diameter Ratio	1.25
Shell Diameter	55 mm
Number of Baffles	14
Inlet and Outlet Baffle Spacing	100 mm
Baffle Spacing	27.46 mm
Baffle Cut	31%

3. MATERIALS AND METHODOLOGY

In the present investigation, an analytical methodology is used for a detailed analysis of STHX. Flow conditions used for the analysis are given in **Table 2**. Details about the methodology are explained in subsequent sections.

Table 2: Flow conditions used for the present investigation

Parameters	**Magnitude/ Description**
Tube side and shell side fluid	Water
Hot fluid temperatures	50°C,70°C, and 90°C
Cold fluid temperatures	30°C
Re on tube side	1000
Re on shell side	1000-5000

The stepwise procedure for theoretical analysis (calculate performance parameters like effectiveness, heat load, and pressure drop) of STHX is given below.

3.1 Calculation of tube side heat transfer coefficient and pressure drop

For a given value of mass flow rate of the fluid, Nu can be expressed as,

$$Nu_t = \frac{(f/2)Re_b Pr_b}{1.07+12.7\left(\frac{f}{2}\right)^{\frac{1}{2}}(Pr_b{}^{2/3}-1)} \tag{1}$$

$$f = (1.58 lnRe - 3.28)^{-2} \tag{2}$$

The heat transfer coefficient on the inner side can be calculated from Eq (03)

$$h_i = \frac{Nu_t \times k_h}{d_i} \tag{3}$$

The tube-side pressure drop can be expressed as,

$$\Delta p_t = 4f \frac{LN_p}{d_i} \rho \frac{u_m{}^2}{2} \tag{4}$$

3.2 Calculation of shell side heat transfer coefficient and pressure drop

Shell side heat transfer coefficient can be calculated from Eq (05),

$$h_o = h_{id} J_c J_l J_b J_s J_r \tag{5}$$

Shell side pressure drop can be calculated from Eq (06),

$$\Delta p_s = [(N_b - 1)\Delta p_{bi} R_b + N_b \Delta p_{wi}] R_l + 2\Delta p_{bi}\left(1 + \frac{N_{cw}}{N_c}\right) R_b R_s \qquad (6)$$

3.3 Calculation of performance parameters

Overall heat transfer coefficient for a clean surface can be calculated from equation (7),

$$U_c = \frac{1}{\frac{d_o}{d_i \times h_i} + \frac{d_o ln\,(\frac{d_o}{d_i})}{2k} + \frac{1}{h_o}} \qquad (7)$$

Effectiveness can be calculated from equation (8),

$$\varepsilon = \frac{2}{1 + C^* + (1 + C^{*2})^{1/2} \frac{1 + exp\left[-NTU\left(1 + C^{*2}\right)^{1/2}\right]}{1 - exp\left[-NTU\left(1 + C^{*2}\right)^{1/2}\right]}} \qquad (8)$$

Outlet temperature of hot fluid can be found using equation (9),

$$T_{h_o} = T_{h_i} - \frac{(\varepsilon \times C_{min}) \times (T_{h_i} - T_{c_i})}{C_{max}} \qquad (9)$$

Outlet temperature of cold fluid is found from equation (10),

$$T_{c_o} = T_{c_i} + (\left(\frac{C_h}{C_c}\right) \times \left(T_{h_i} - T_{h_o}\right)) \qquad (10)$$

Heat recovery is found from Eq (11),

$$Q = C_h \times \left(T_{h_i} - T_{h_o}\right) \qquad (11)$$

4. RESULTS AND DISCUSSION

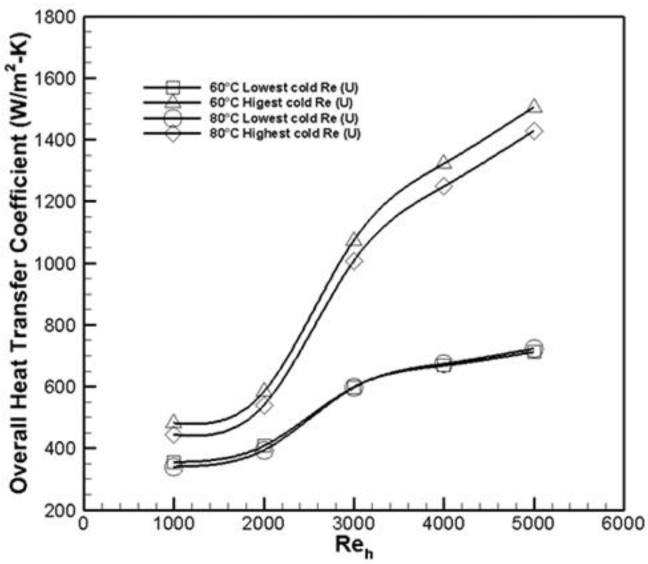

Figure 1: Effect of Re of hot fluid on overall heat transfer coefficient of the heat exchanger at various inlet temperatures of the hot fluid.

Fig. 1 shows the variation in the overall heat transfer coefficient for Re of the hot fluid ranging from 1000 to 5000 for different inlet temperatures of the hot fluid. Two inlet temperatures of the hot fluid are taken - 60°C and 80°C. The lowest cold Re indicates that the Re of the cold fluid for that particular trendline has been assumed as 1000 and the highest cold Re indicates that the Renolds number of the cold fluid is assumed as 5000. It can be observed that at any inlet temperature of the hot fluid, the overall heat transfer coefficient increases with an increase in the Re of the hot fluid. This is because the heat capacity of the hot fluid increases as increasing the Re indicates a direct increase in the mass flow rate of the fluid. We can also observe that from

Re = 1000 to Re = 2000 there is a gradual increase in Re and then after Re = 2000 there is a sudden increase in Re. This is because from Re = 2000 to Re = 3000 the fluid is in a transition phase where the fluid is neither laminar nor turbulent. Further, we can also see that at a constant value of Re of the hot fluid, a higher overall heat transfer coefficient is observed for a higher inlet temperature of the hot fluid. This is so as the heat capacity of the fluid increases with an increase in the inlet temperature of the hot fluid.

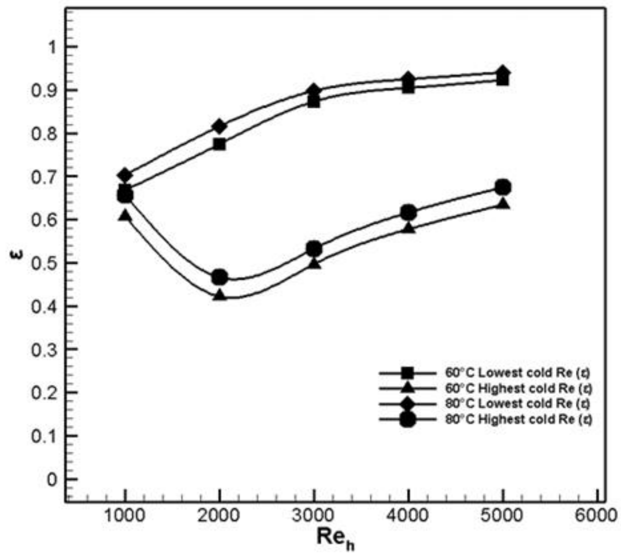

Figure 2: Effect of Re of hot fluid on effectiveness of heat exchanger at various inlet temperatures of the hot fluid.

Fig. 2 shows variation in effectiveness for Re of the hot fluid ranging from 1000 to 5000 for different inlet temperatures of the hot fluid. It is seen that at any inlet temperature of the hot fluid, the effectiveness of the heat exchanger decreases, attains a minimum value, and then rises again for a low value of Re of the cold fluid. This is because initially when the Re of the hot fluid is low the value of heat capacity is less than 1. As the Re of hot fluid increases the heat capacity increases and as soon as its value is greater than 1 the effectiveness starts increasing. An opposite trend is observed when the Re of the cold fluid is highest. The effectiveness continuously increases with an increase in Re of the hot fluid for any inlet temperature of the hot fluid.

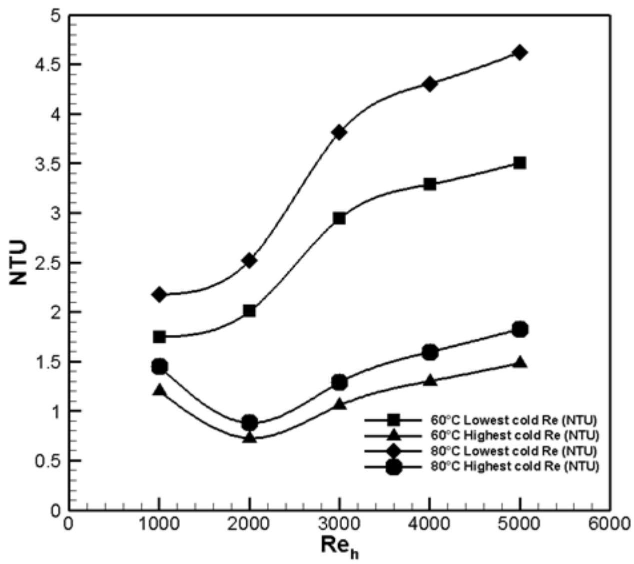

Figure 3: Effect of Re of hot fluid on NTU of heat exchanger at various inlet temperatures of the hot fluid.

Fig. 3 shows the variation of NTU for Re of the hot fluid ranging from 1000 to 5000 for different inlet temperatures of the hot fluid. It can be observed that at a higher value of Re of cold fluid the NTU first decreases reaches a minimum value and then increases similar to the trend observed in effectiveness. This is so because NTU is directly correlated to effectiveness. When the Re of cold fluid is assumed to be 1000 the NTU shows an increasing trend for an increase in Re of hot fluid for any inlet temperature of the hot fluid.

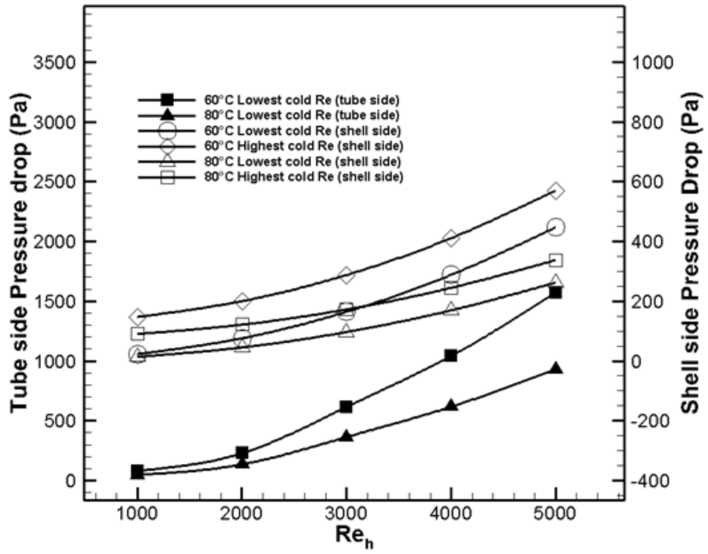

Figure 4: Effect of Re of hot fluid on tube side and shell side pressure drop of the heat exchanger at various inlet temperatures of the hot fluid.

Fig. 4 shows the variation of tube side and shell side pressure drop for Re of the hot fluid ranging from 1000 to 5000 for different inlet temperatures of the hot fluid. It can be observed that a greater pressure drop is observed on the tube side as compared to the shell side. We observe that as the Re of the hot fluid increases, the pressure drop on both the shell side and tube side also increases. This is so because the pressure drop is directly proportional to the velocity of flow. A higher Re indicates a higher mass flow rate of the fluid. A higher mass flow rate of the fluid shows a higher mean velocity of flow and hence a higher pressure drop.

CONCLUSION

The present study focuses on the theoretical analysis of performance parameters of a shell and tube heat exchanger. A theoretical model was developed for analysis of the thermal and hydraulic characteristics of the STHX at various inlet conditions. The effect of Re of hot fluid on the thermohydraulic characteristics is investigated theoretically. A summary of the results drawn based on the present work is summarized in this section. It was observed that the overall heat transfer coefficient and the tube side pressure drop have a direct correlation with the Re for the fluid on the hot side. This is obvious from the fact that both these characteristics have a direct dependence on the velocity of the fluid and Re is a function of fluid velocity. It is also observed that at any inlet temperature of the hot fluid, the effectiveness of the heat exchanger decreases, attains a minimum value, and then rises again for a low value of Re of the cold fluid. In the case of NTU for a heat exchanger, it can be observed that at a higher value of Re of cold fluid the NTU first decreases reaches a minimum value, and then increases similar to the trend observed in effectiveness. This is so because NTU is directly correlated to effectiveness.

Conflict of Interest

On behalf of all the authors, the corresponding author states that there is no conflict of interest.

REFERENCES

[1] B.I. Master, K.S. Chunangad, V. Pushpanathan, Fouling mitigation using helixchanger heat exchangers, Proceedings of the ECI Conference on Heat Exchanger Fouling and Cleaning: Fundamentals and Applications, May 18-22,2003, Santa Fe, NM, pp. 317e322.

[2] H.R. Abbasi, E.S. Sadeh, H. Pourrahmani, M.H. Mohammadi, Shape optimization of segmental porous baffles for enhanced thermo-hydraulic performance of shell and tube heat exchanger Applied Thermal Engineering 180 (2020) 115835.

[3] N. Afsar, M.I. Inam, CFD analysis of shell and tube heat exchanger with different baffle orientation and baffle cut AIP Conference Proceedings 1980 (2018) 050006.

[4] N. Bicer, T. Engin, H. Yasar, E. Buyukkaya, A. Aydin, A. Topuz, Design optimization of a shell and tube heat exchanger with novel three-zonal baffle using CFD and taguchi method International Journal of Thermal Sciences 155 (2020) 106417.

[5] P. Bichkar, O. Dandgaval, R. Godase, T. Dey, Study of shell and tube heat exchanger with the effect of types of baffles Procedia Manufacturing 20 (2018) 195-200.

[6] A. Karno, S. Ajib, Effect of tube pitch on heat transfer in shell and tube heat exchangers-new simulation software Heat and Mass Transfer 42 (2006) 263-270.

[7] M.I. Kim, Y. Lee, B.W. Kim, D.H. Lee, W.S. Song, CFD modelling of shell and tube heat exchanger header for uniform distribution among tubes Korean Journal of Chemical Engineering 26 (2) (2007) 359-363.

[8] G.B. Leoni, T.S. Klein, R.A. Medronho, Assessment with computational fluid dynamics of the effects of baffle clearances on the shell side flow in a shell and tube heat exchanger Applied Thermal Engineering 112 (2017) 597-506.

[9] Y.G. Lei, Y.L. He, P. Chu, R. Li, Design and optimization of heat exchangers with helical baffles, Chemical Engineering Science 63 (2008) 4386-4395.

[10] M. Mellal, R. Benzeguir, D. Sahel, H. Ameur, Hydro-thermal shell-side performance evaluation of a shell and tube heat exchanger under different baffle arrangement and orientation, International Journal of Thermal Sciences 121 (2017) 138-149.

[11] E. Ozden, I. Tari, Shell side CFD analysis of a small shell and tube heat exchanger Energy Conversion and Management 51 (2010) 1004-1014.

[12] S. Kallannavar, S. Mashyal, M. Rajangale, Effect of tube layout on the performance of shell and tube heat exchangers Materials Today: Proceedings 27 (1) (2020) 263-267.

[13] J. Mahendran, Experimental analysis of shell and tube heat exchanger using flower baffle plate configuration Materials Today: Proceedings 21 (1) (2020) 419-424.

[14] J. Chen, X. Lu, Q. Wang, M. Zeng, Experimental investigation on thermal-hydraulic performance of a novel shell and tube heat exchanger with unilateral ladder type helical baffles Applied Thermal Engineering 161 (2019) 114099.

[15] N. Li, J. Chen, T. Cheng, J.J. Klemes, P.S. Varbanov, Q. Wang, W. Yang, X. Liu, M. Zeng, Analyzing thermal-hydraulic performance and energy efficiency of shell-and-tube heat exchangers with longitudinal flow based on experiment and numerical simulation Energy 202 (2020) 117757.

[16] S.A. Marzouk, M.M. Abou Al- Sood, E.M.S. El-Said, M.K. El-Fakharany, Effect of wired nails circular-rod inserts on tube side performance of shell and tube heat exchanger: Experimental study Applied Thermal Engineering 167 (2020) 114696.

[17] K. Kannan, R. Rudramoorthy, Experimental and Numerical Analysis of Laminar and Low Turbulent Flow Distributions in Inlet Dividing Header of Shell and Tube Heat Exchanger Journal of Hydrodynamics, Ser. B 22 (4) (2010) 494-502.

[18] J.F. Yang, Y.S. Lin, H.B. Ke, M. Zeng, Q.W. Wang, Investigation on combined multiple shell-pass shell and tube heat exchanger with continuous helical baffles Energy 115 (3) (2016) 1572-1579.

[19] H. Li, V. Kottke, Visualization and determination of local heat transfer coefficients in shell and tube heat exchangers for staggered tube arrangement by mass transfer measurements Experimental and Thermal Fluid Science 17 (1998) 210-216.

[20] S. Wang, J. Wen, H. Yang, Y. Xue, H. Tuo, Experimental investigation on heat transfer enhancement of a heat exchanger with helical baffles through blockage of triangle leakage zones, Applied Thermal Engineering 67 (2014) 122-130.

[21] B. Peng, Q.W. Wang, C. Zhang, G.N. Xie, L.Q. Luo, Q.Y. Chen, M. Zeng, An experimental study of shell and tube heat exchangers with continuous helical baffles ASME Journal of Heat Transfer 129 (2007) 1425-1431.

[22] F.P. Incropera, D.P. Dewitt, Introduction to Heat Transfer, Wiley, 1996.

[23] D.Q. Kern, Process Heat Transfer, International Student Edition, McGraw-Hill International Book Company, 21st Edition, 1983.

[24] S. Kakac, H. Liu, A. Pramuanjaroenkij, Heat Exchangers Selection, Rating and Thermal Design, Third Edition, CRC Press, 2012.

[25] E. Cao, Heat Transfer in Process Engineering, First Edition, The McGraw- Hill Companies, 2010.

[26] E.U. Schlunder, Heat Exchanger Design Book, Taylor and Francis Inc, Hemisphere Publishing Corporation, 1983.